HHS Public Access

Author manuscript

Exp Eye Res. Author manuscript; available in PMC 2021 December 01.

Published in final edited form as:

Exp Eye Res. 2020 December ; 201: 108296. doi:10.1016/j.exer.2020.108296.

Single transient intraocular pressure elevations cause prolonged retinal ganglion cell dysfunction and retinal capillary abnormalities in mice

Xiaofeng Tao[a], **Rohini R. Sigireddi**[a], **Peter D. Westenskow**[a,#], **Roomasa Channa**[a], **Benjamin J. Frankfort**[a,b,*]

[a]Department of Ophthalmology, Baylor College of Medicine

[b]Department of Neuroscience, Baylor College of Medicine

Abstract

Transient intraocular pressure (IOP) elevations are likely to occur in certain forms of glaucoma and after intravitreal injections to treat various retinal diseases. However, the impact of these transient IOP elevations on the physiology of individual retinal ganglion cells (RGCs) is unknown. In this report, we explore how transient IOP elevations in mice affect RGC physiology, RGC anatomy, and retinal arteriole and capillary structure. Transient IOP elevation was induced in 12-week old wild type C57BL6J mice by injecting sodium hyaluronate into the anterior chamber. IOP was measured immediately after the injection and again 1 and 7 days later. Average peak IOP after injection was ~50 mmHg and subsequent IOPs returned to normal. RGC physiology was assessed with a multielectrode array (MEA) by calculating a spike triggered average (STA) at the same time points. RGC counts and retinal vascular structure were assessed 14 days after injection with immunohistochemistry to label RGCs and blood vessels. Transient IOP elevation caused a marked reduction of scotopic STA presence and delayed center and surround STA peak times that did not recover. Transient IOP elevation also caused a reduced photopic receptive field size and spontaneous firing rate, both of which showed some recovery with time. Transient IOP elevation also induced vascular remodeling: the number of capillary branches was decreased within the superficial and intermediate vascular plexi. RGC counts, retinal arteriole diameter, and deep capillary plexus branching were unaffected. These previously unappreciated findings suggest that transient IOP elevation may cause unrecognized and potentially long-term pathology to RGCs and associated neurovascular units which should be accounted for in clinical practice.

[*]Author for Correspondence: Benjamin J. Frankfort, M.D., Ph.D., Department of Ophthalmology, Baylor College of Medicine, 6565 Fannin St, NC – 205 Houston, TX 77030 benjamin.frankfort@bcm.edu.

[#]Current address: F. Hoffman-La Roche, Ophthalmology, I2O, Grenzacherstrasse 124, 4070 Basel, Switzerland

Conflict of interest statement

The authors have no financial of competing interest related to this work. All authors approved the final version of the manuscript.

Keywords

Intraocular pressure; IOP; Transient IOP elevation; Retinal ganglion cell; RGC; Retinal vasculature

1. Introduction

In humans, sustained elevations in intraocular pressure (IOP) to high levels are seen in a number of secondary glaucomas and may lead to permanent visual disability due to injury to retinal ganglion cells (RGCs) and their axons at the optic nerve head. However, the effects of transient IOP elevation to high levels are less clear. One common cause of transient IOP elevation is appositional closure of the anterior chamber angle. This condition can cause intermittent visual symptoms such as blurred vision, haloes, and focal headaches due to IOP elevations, and potentially progress to primary angle closure glaucoma (Aung et al., 2004; Devereux et al., 2000; Thomas et al., 2003).

The most common cause of transient IOP elevation in humans, though, is iatrogenic. Intravitreal injections of anti-Vascular Endothelial Growth Factor (anti-VEGF) agents are the primary treatment for several diseases which are defined by neovascularization or macular edema (Tah et al., 2015). Specific data about IOP level following anti-VEGF injection in humans varies in its collection and presentation, but there is universal agreement that the procedure causes acute IOP elevation. Indeed, when measured within one minute of injection, all patients have an increase in IOP (Cacciamani et al., 2013; Gregori et al., 2014; Hariprasad et al., 2006; Hong and Jee, 2012; Knip and Valimaki, 2012; Murray et al., 2014; Pang et al., 2015a). This increase is not subtle, and several studies report post-injection mean IOP levels of > 40 mmHg, ranging from 41.2 mmHg to 47.1 mmHg, with a pre-injection IOP of ~15 mmHg (Gregori et al., 2014; Hong and Jee, 2012; Knip and Valimaki, 2012; Murray et al., 2014). These IOP elevations are transient, normalizing in most cases within one hour (Knip and Valimaki, 2012). The specific impact of repeated elevations of IOP on optic nerve health is not completely understood, although there is at least some evidence for progressive loss of retinal nerve fiber layer with repeated anti-VEGF injections in humans (Martinez-de-la-Casa et al., 2012).

Electrophysiologic testing in a variety of animal species have been used to determine the functional impact of acute experimental IOP elevation to high levels. In rats, electroretinogram (ERG) studies consistently find that retinal cell types show differential susceptibility to IOP-induced dysfunction. RGCs are most sensitive to acute IOP elevation and become dysfunctional even at sub-ischemic levels (Bui et al., 2005; Bui et al., 2013; Tan et al., 2018). RGCs are also susceptible to cumulative damage from repeat IOP elevations (He et al., 2008). Outer retinal cell types such as bipolar cells and photoreceptors become dysfunctional at higher levels of IOP (Bui et al., 2005; Sun et al., 2007; Tan et al., 2018) and recover more quickly than RGCs after discontinuation of IOP elevation (He et al., 2006). Furthermore, scotopic pathways are more sensitive to injury than are photopic pathways (Tsai et al., 2014), a finding that also occurs in cats (Uenoyama et al., 1969). Studies in mice confirm ERG findings after IOP elevation, and show that RGCs display delayed recovery

from even a single IOP spike (Kong et al., 2009). Consistent with these ERG studies, we have previously shown in mice that sub-ischemic transient IOP elevations induced by injection of sodium hyaluronate to the anterior chamber have dramatic effects on optokinetic contrast sensitivity, particularly under dark (scotopic) conditions (van der Heijden et al., 2016). We revisited this model to assess the physiologic effects of single, transient, acute IOP elevations on RGC physiology at the single RGC level, as well as the retinal capillary vasculature. We found that transient sub-ischemic IOP elevations caused profound effects on RGC physiology, not all of which recovered with time, as well as vascular remodeling of specific capillary plexi, all in the setting of normal and unchanged RGC numbers.

2. Materials and Methods

2.1. Experimental animals

Animals used in this study were 12-week old wild type C57BL/6J mice of both genders (Jackson Laboratories, stock No. 000664). 69 mice were used in the study: 42 for electrophysiologic experiments, 17 for histologic investigation, and 10 to determine the pattern of acute IOP elevation in the first 12 hours. All animals were kept at Baylor College of Medicine facilities and were cared for by a dedicated veterinarian team. Animal treatments were approved by the Institutional Animal Care and Use Committee of Baylor College of Medicine, and in accordance with U.S. statutes for the use of laboratory animals and the ARVO statement for the use of animals in ophthalmic and vision research.

2.2. Transient intraocular pressure elevation

All animals were initially pre-screened for normal IOP (approximately 7–12 mmHg) and general eye health. IOP was measured under isoflurane anesthesia with a rebound tonometer (Icare Finland OY, Vantaa, Finland), and the result was an average of at least 6 repeated measurements. All IOP measurements were taken within a short time window (10am – 2pm) to minimize diurnal IOP changes. A set of established procedures was used to create transient IOP spikes (van der Heijden et al., 2016). Briefly, systemic anesthesia was induced and maintained by allowing the animal to breath a mixture of isoflurane and oxygen. Topical anesthesia was achieved with a 0.5% proparacaine drop on the cornea. When adequate anesthesia was confirmed, a corneal puncture was made in one eye with a sterile 30-gauge needle. This incision was used to insert a glass micropipette attached to a tube of highly viscous sodium hyaluronate (Healon 5, Abbott Medical Optics, Abbott Park, IL, USA). Sodium hyaluronate was injected into the anterior chamber until a small reflux occurred. IOP was measured immediately following the injection (D0) and again on day 1 (D1) and day 7 (D7). A total of 45 mice underwent acute IOP elevation. 27 mice were used for physiologic experiments (9 on D0, 8 on D1, and 10 on D7), 8 mice were used for histologic experiments, and 10 mice were used to determine the pattern of acute IOP elevation in the first 12 hours (Supplemental Figure 1). 15 control animals for physiologic studies were age-matched and did not receive any injection. 9 control animals for histologic experiments received an injection of a 1.5 μL PBS (saline) followed by 3 μL sodium hyaluronate (Provisc, Alcon, Ft. Worth, TX, USA) as previously described (Frankfort et al., 2013) to allow for intra-animal, inter-retinal comparisons.

2.3. Multielectrode array (MEA) recording

Before being euthanized for MEA recording, all animals were dark-adapted for at least 2 hours. The MEA procedures followed an established protocol (Sabharwal et al., 2017; Tao et al., 2019). Briefly, after euthanasia and enucleation, the neural layers of the retina were surgically isolated in a carboxygenated buffer (NaCl 124mM, KCl 2.5mM, $CaCl_2$ 2mM, $MgCl_2$ 2mM, NaH_2PO_4 1.25mM, $NaHCO_3$ 26mM, glucose 22mM, pH titrated to 7.35, bubbled with 95% O_2 and 5% CO_2) under infrared illumination (B.E. Meyers & Co., Inc., Redmond, WA), and flat-mounted on a pigmented micro-filter membrane (EMD Millipore, Burlington, MA). The retina and the membrane were transferred to the array (MEA-60, Multichannel System MCS GmbH, Reutlingen, BW, Germany) with the optic nerve placed approximately on the center of array, where it was continuously perfused with the dissection buffer. The array was kept at a constant temperature (36.5ºC) with an on-stage heating element and the perfused solution was heated with an in-line heater. The retina was allowed to sit in the array for 15–30 min to recover from the stress sustained from the isolation procedures before beginning the experiments. Experiments were started when reliable spontaneous RGC activities were observed. Spikes were collected from 60 electrodes of the array. Spiking signals were acquired at 20KHz and passed through a 0.1Hz high-pass digital filter for real time feedback. Raw data was processed off-line in MATLAB (MathWorks Inc., Natick, MA) for spike sorting and other analysis.

Ambient light calibration was as previously described (Tao et al., 2019). A digitally controlled filter wheel (Edmund Optics Inc., Barrington, NJ) was used to add or remove neutral density filters in the light pathway. An OLED microdisplay (eMagin Inc., Hopewell Junction, NY) was used to display visual stimuli. Images on the microdisplay was optically projected to the entire retina through a beam splitter (Edmund Optics Inc., Barrington, NJ). All recordings started from scotopic stimulation, followed by photopic stimulation.

Visual stimuli consisted of a series of 32×32 binary (black and white) checkerboards (total 20,625 frames) presented to the retina at a refresh rate of 15Hz. Each element of the checkerboards was a white or black square of 50μm on its side, flickering at 15Hz. These checkerboards were generated in PsychToolbox and were displayed for about 90 minutes at scotopic and photopic lighting level, respectively. Collected RGC spikes were later reverse-correlated to the checkerboard frames for the calculation of space-time STAs (Chichilnisky, 2001; Meister et al., 1994).

To characterize RGC contrast responses, a whole-field stimulation with 18 different contrast levels was used. These contrast levels ranged from 2.4% to 92% and were presented in a pseudorandom order. At each contrast level, light intensity of the microdisplay changed sinusoidally about a mean background (a grey screen) at 2Hz and last for 15 seconds. There was a 5 second inter-stimulation interval preceding each trial. The whole set of the contrast levels was repeated twice.

A whole-field dark (black) or bright (white) stimulation was used to identify RGC polarity. Alternating, uniform black or white screens were displayed for 4 seconds and the cycle was repeated 12 times. This stimulation was under photopic ambient light only.

Spikes were also collected when the retina was under scotopic ambient light and was not visually evoked by any stimulus. These spikes were considered to be the spontaneous or baseline firing of the RGCs.

Data analysis were performed off-line in MATLAB. The ON/OFF polarity of the RGCs was determined as previously described (Tao et al., 2019). STAs were fit to a model that consisted of a 2D spatial Gaussian and the impulse response of a temporal filter (Chichilnisky and Kalmar, 2002). Fitting quality was evaluated with an r^2 calculated from the entire 32×32 space-time map. All the RGCs that had a well-defined ON/OFF response pattern and r^2 of the STA over 0.3 were included for subsequent analysis that aimed to characterize its receptive field's (RF's) spatial and temporal properties. Population characteristics of these properties were expressed both by mean ± SEM and a kernel density estimation curve (calculated with built-in MATLAB function *ksdensity*) to illustrate its distribution.

More than two thirds of the RGCs (713 out of 1075) responded well to contrast modulation. In these cells, firing rates were fit to a Naka-Rushton function as previously described (Tao et al., 2019) and plotted as a function of contrast level.

2.4. RGC counting and measurement of retinal vasculature

Both eyes of the same mouse were prepared in parallel to ensure that all intra-animal, inter-retina comparisons were maximally controlled. Eyes were isolated at ~2 weeks after IOP elevation, fixed, and blocked as previously described (Frankfort et al., 2013). Eyes were stained with Isolectin GS-IB_4 conjugated to Alexa Fluor 488 (1:200, ThermoFisher) and guinea pig anti-RBPMS (1:300, PhosphoSolutions) followed by donkey anti-guinea pig Cy3 as the secondary antibody (1:300, Jackson ImmunoResearch) (Almasieh et al., 2013; Rodriguez et al., 2014; Usui et al., 2015). After mounting, whole mount retinas were imaged with a Zeiss LSM 810 series confocal microscope. RBPMS positive cells imaged from four positions located 50% from the optic nerve head were manually counted and then averaged to determine the RGC number per unit area as previously described (Frankfort et al., 2013).

Retina vasculature was quantified as follows. First, the retina was imaged at low (10x) power using confocal microscopy. A circle measuring 1.5mm which was centered on the optic nerve was placed on this image to define the mid-retina intersection points of each arteriole (4–7) for further study. This approach ensured that the RGCs studied with the MEA were contained within the circle used to study the vasculature. Second, at higher (20x) power, the arterioles at each intersection were imaged and their diameter measured. Third, a Z-stack image through the entire retinal capillary structure adjacent to the intersection point of each arteriole was taken. Fourth, offline images were assessed in ImageJ using the FIJI extension to determine the delineation of the superior, intermediate, and deep capillary plexi and to manually count the number of capillary branch points for each plexus. Fifth, arteriole diameter and retinal capillary branches were averaged for each arteriole location to generate a composite number across the entire retina (Kurihara et al., 2010; Usui et al., 2015). Sixth, the averaged numbers for the injected experimental eye (transient IOP elevation or saline) of each mouse was compared to the averaged numbers of the uninjected control eye of the

same mouse to express the experimental eye as a percentage of the intra-animal control (experimental/control x 100).

2.5. Experimental design and statistics

All physiologic data were presented with means and SEMs in the figures. ANOVA with Fisher's LSD post-hoc statistics was used to test the significance ($\alpha = 0.05$) of all comparisons including all Figures and Tables except for the retinal vasculature and RGC numbers in Table 3 which were compared with a t test ($\alpha = 0.05$).

3. Results

3.1. IOP elevation

In all experimental eyes for physiology (n = 27), injection of sodium hyaluronate produced a transient IOP elevation (IOP = 49.35±1.35 mmHg; pre-injection IOP = 8.79±0.24 mmHg; mean±SEM). 9 eyes were used for immediate experiments and the remaining 18 eyes which were analyzed at later time points returned to baseline levels of IOP (8.23±0.30 mmHg) at 24 hours and remained normal (8.18±0.39 mmHg) after 7 days (Table 1). 10 additional animals were injected to determine the pattern of acute IOP elevation in the first 12 hours, and IOP returned to baseline within 1 hour (Supplemental Figure 1).

3.2. Changes in retinal ganglion cell physiology

The number of retinas and RGCs studied physiologically at each time point and for control animals are listed in Table 2. Transient IOP elevation caused a marked reduction in scotopic responses and scotopic STAs were identified in only 1% of the RGCs at D0. This increased to 13% at D1 and 6% at D7, all significantly lower compared to that in control population (26%; $p<0.01$ by chi-square test, degree of freedom adjusted; Figure 1A). This paucity of scotopic responses limited further analysis and discussion exclusively to RGC photopic responses.

RGC spontaneous firing rate was reduced from 2.3Hz to 1.5Hz at D0, a more than 30% drop ($p<0.001$; Figure 1B). There was rapid partial recovery of RGC spontaneous activity with a return to normal IOP level by D1 (1.7Hz; still lower than control, $p<0.01$), but no further recovery by D7 (1.8Hz; still lower than control, $p<0.05$).

We next explored the effects of transient IOP elevation on the spatial and temporal characteristics of RGC center receptive fields (RFs) under photopic light. The average RF size was 74.0±0.6 μm in control RGCs, which was reduced to 71.1±1.0 μm at D0 (Figure 2A; $p<0.05$). However, RF size fully recovered and even increased in size compared to control by D1 (77.9±1.2 μm; $p<0.01$). This increased RF size did not persist at D7 (76.3±1.3 μm). Temporal properties were strongly affected by transient IOP elevation, which caused a marked delay in center STA peak time at all time points. The center STA peak time increased to 136.1±2.1 msec at D0, from a baseline of 110.5±0.9 msec (Figure 2B; $p<0.001$). This delay in peak time persisted at later time points, with no trend of recovery at D1 (131.7±2.7 msec) or D7 (136.5±2.7 msec; both $p<0.001$ compared to control).

RF surround was also severely impacted by transient IOP elevation, as a substantial portion of the RGCs completely lost antagonistic surround (Figure 3A). In control RGCs, antagonistic surround was present in more than 77% of the population. This ratio dropped to 32% - 48% after transient IOP elevation ($p<0.001$ for all three time points). We calculated the surround STA peak time for the minority of RGCs in which antagonistic surround was still present. The surround STA peak time showed an elongation pattern that was similar to the center STA peak time (Figure 3B). Indeed, transient IOP elevation extended the surround STA peak time from 175.8±3.1 msec to 198.0±4.3 msec at D0, with no recovery and possibly further decline at D1 (215.2±8.2 msec) and D7 (207.7±6.7 msec; $p<0.001$ for all 3 time points).

Finally, we examined photopic contrast sensitivity of RGCs following transient IOP elevation (Figure 4). No strong effects on contrast sensitivity were seen at any time points, suggesting that this property was resistant to transient IOP elevations.

3.3. Changes in retinal anatomy

To explore possible mechanisms underlying these physiological changes, we conducted immunohistochemical studies on additional retinas that were subjected to the same injection procedures (average IOP = 51.88 ± 2.93 mmHg for sodium hyaluronate eyes [n = 8] and IOP = 9.32 ± 0.23 mmHg for control eyes [n = 9]; Table 1; see Methods). Consistent with our previous study, transient IOP elevation had no effect on RGC numbers, suggesting that a single transient IOP elevation to this level was insufficient to cause RGC loss (Table 3) (van der Heijden et al., 2016). We explored additional potential effects of transient IOP elevation by analyzing the retinal vasculature (Table 3). While retinal arteriole diameter was unaffected by IOP elevation, a prominent effect was seen on the capillary microvasculature (Figure 5). Here, a single transient IOP elevation caused a reduction of both superficial and intermediate plexus branching (82%±18% and 88%±14% of control branches, respectively), but spared the branches of the deep plexus (98%±13% of control branches).

4. Discussion

In this manuscript, we produced transient, acute, sub-ischemic IOP elevation in mice with sodium hyaluronate injection and examined RGC function at the single cell level. We uncovered a number of physiologic changes that occurred immediately with IOP elevation. Interestingly, while some of these changes recovered fully (RF size) or partially (spontaneous firing rate) with a return to normal levels of IOP, others were persistently abnormal as far as one week after the initial IOP elevation (proportion of RGCs with a scotopic STA, delay in center and surround STA peak times). Other RGC properties (photopic contrast sensitivity) were resistant to the effects of transient IOP elevations. We then explored retinal anatomy and found that while RGC counts remained normal following IOP elevation, the number of retinal capillary branches was decreased specifically within the superficial and intermediate plexi. Together, these findings implicate a persistent IOP effect on both RGCs and upstream horizontal circuits, most likely amacrine cells, even after a single IOP elevation.

Scotopic pathways are primarily dependent on intact amacrine cell networks to transmit visual information from rods to RGCs (Arman and Sampath, 2012; Ivanova et al., 2006; Kolb and Famiglietti, 1974; Pang et al., 2007; Strettoi et al., 1990; Trexler et al., 2005). Furthermore, RGC/amacrine cell interactions underlie some of the temporal properties of RGC responses (Ke et al., 2014; Pang et al., 2004; Sabharwal et al., 2016). Thus, the near complete loss of scotopic STAs and the marked temporal delay of both center and surround RF peak times after a single transient IOP elevation strongly suggest that dysfunctional amacrine cells contribute to these observations (Cowan et al., 2016). The observation in other animal models that amacrine cells are quite sensitive to effects of IOP elevation supports this interpretation (Akopian et al., 2017; Akopian et al., 2019; Frankfort et al., 2013; Pang et al., 2015b; Sabharwal et al., 2017). This interpretation may also explain the relative susceptibility of scotopic pathways to IOP in various ERG studies (Tsai et al., 2014; Uenoyama et al., 1969). Furthermore, amacrine cells form a neurovascular unit with the capillaries of the intermediate plexus, and post-development ablation of amacrine cells leads to a secondary loss of intermediate plexus capillary branches, similar to our findings in this study (Usui et al., 2015). Interestingly, the lack of recovery of amacrine cell mediated RGC physiologic properties after IOP normalized implicates a slowly reversible or irreversible mechanism which is again consistent with prior ERG studies (Kong et al., 2009). While plausible that a single IOP elevation could cause a direct and long-lasting effect on amacrine electrical properties, it is also possible that this mechanism is indirect, and involves a persistent abnormality of non-neuronal cells (such as retinal capillaries) even as amacrine cells themselves recover. Additional experiments to directly assess amacrine cell function or to prevent capillary losses would be helpful to discern between these possibilities.

RGCs themselves are also likely to be directly impacted by transient IOP elevations, but not all RGC properties were equally affected in this study. For example, photopic contrast sensitivity was not affected by IOP elevation, and we did not see a reduction in RGCs after IOP elevation, suggesting a relative resistance of contrast detection and cell survival to a single IOP elevation. In contradistinction, the RGC neurovascular unit, which includes RGC dependent regulation of the superficial vascular plexus, appears to be more sensitive to transient IOP elevation (Edwards et al., 2012; Okabe et al., 2014; Sapieha et al., 2008). Somewhere in the middle lies the spontaneous firing rate – acutely reduced with partial recovery following IOP elevation. These findings are consistent with our current understanding of RGCs – they are capable of integrating multiple properties with distinct IOP thresholds simultaneously (Sabharwal et al., 2017; Tao et al., 2019). Additional experiments at a wider range of IOPs would help define these thresholds with greater certainty.

The primary limitation of this study is that IOP was measured in anesthetized mice. Since anesthesia can reduce IOP levels in rodents (Jia et al., 2000), it is likely that the true levels of IOP in this study are actually higher than what was measured. Since the IOP levels achieved in the study were already on the upper end of those seen after anti-VEGF injection (Hoguet et al., 2019), it is therefore possible the IOP achieved in this study is higher than what is seen in patients. However, the time course of IOP elevation is consistent with the clinical situation.

Despite this caveat, the study has several potential clinical implications. As RGC and amacrine cell physiology are not routinely tracked in the setting of retinal disease, where the acute IOP elevations caused by anti-VEGF intravitreal injections are most common, it is possible that unrecognized dysfunction of the inner retina occurs even as retinal anatomy is improved by anti-VEGF treatments. If so, this may impact visual outcomes. Furthermore, while RGC anatomy was not affected by the single IOP elevations induced in this study, there is evidence for retina nerve fiber layer (RNFL) thinning with repeated anti-VEGF treatments in humans (Martinez-de-la-Casa et al., 2012). While it is not easy to distinguish if the RNFL thinning is caused by the cumulative effect of repeated acute IOP elevations, persistent IOP increases between treatments, or some other effect, it is important to consider the potential impact of exposure to transient IOP elevations among patients who are at higher than normal risk from IOP damage, such as those with known or suspected glaucoma.

Supplementary Material

Refer to Web version on PubMed Central for supplementary material.

Acknowledgments

Thank you to Schuyler Link and Jacob Trachtenberg for assistance counting retinal capillary branch points.

Funding Sources

This work was supported by NIH R01 Grant EY025601 (B.J.F.), NIH Vision Core Grant EY002520 (Baylor College of Medicine), a gift from the Hamill Foundation (Houston, TX, to B.J.F.), and a departmental research grant from Research to Prevent Blindness (New York, NY) to Baylor College of Medicine. The funding sources were not involved in the study design, analysis and interpretation of data, writing of the manuscript, or the decision to publish the article.

References

Akopian A, Kumar S, Ramakrishnan H, Roy K, Viswanathan S, Bloomfield SA, 2017 Targeting neuronal gap junctions in mouse retina offers neuroprotection in glaucoma. J Clin Invest 127, 2647–2661. [PubMed: 28604388]

Akopian A, Kumar S, Ramakrishnan H, Viswanathan S, Bloomfield SA, 2019 Amacrine cells coupled to ganglion cells via gap junctions are highly vulnerable in glaucomatous mouse retinas. J Comp Neurol 527, 159–173. [PubMed: 27411041]

Almasieh M, MacIntyre JN, Pouliot M, Casanova C, Vaucher E, Kelly ME, Di Polo A, 2013 Acetylcholinesterase inhibition promotes retinal vasoprotection and increases ocular blood flow in experimental glaucoma. Invest Ophthalmol Vis Sci 54, 3171–3183. [PubMed: 23599333]

Arman AC, Sampath AP, 2012 Dark-adapted response threshold of OFF ganglion cells is not set by OFF bipolar cells in the mouse retina. J Neurophysiol 107, 2649–2659. [PubMed: 22338022]

Aung T, Friedman DS, Chew PT, Ang LP, Gazzard G, Lai YF, Yip L, Lai H, Quigley H, Seah SK, 2004 Long-term outcomes in asians after acute primary angle closure. Ophthalmology 111, 1464–1469. [PubMed: 15288972]

Bui BV, Edmunds B, Cioffi GA, Fortune B, 2005 The gradient of retinal functional changes during acute intraocular pressure elevation. Invest Ophthalmol Vis Sci 46, 202–213. [PubMed: 15623775]

Bui BV, He Z, Vingrys AJ, Nguyen CT, Wong VH, Fortune B, 2013 Using the electroretinogram to understand how intraocular pressure elevation affects the rat retina. J Ophthalmol 2013, 262467.

Cacciamani A, Oddone F, Parravano M, Scarinci F, Di Nicola M, Lofoco G, 2013 Intravitreal injection of bevacizumab: changes in intraocular pressure related to ocular axial length. Jpn J Ophthalmol 57, 63–67. [PubMed: 23093311]

Chichilnisky EJ, 2001 A simple white noise analysis of neuronal light responses. Network 12, 199–213. [PubMed: 11405422]

Chichilnisky EJ, Kalmar RS, 2002 Functional asymmetries in ON and OFF ganglion cells of primate retina. J Neurosci 22, 2737–2747. [PubMed: 11923439]

Cowan CS, Sabharwal J, Wu SM, 2016 Space-time codependence of retinal ganglion cells can be explained by novel and separable components of their receptive fields. Physiol Rep 4.

Devereux JG, Foster PJ, Baasanhu J, Uranchimeg D, Lee PS, Erdenbeleig T, Machin D, Johnson GJ, Alsbirk PH, 2000 Anterior chamber depth measurement as a screening tool for primary angle-closure glaucoma in an East Asian population. Arch Ophthalmol 118, 257–263. [PubMed: 10676792]

Edwards MM, McLeod DS, Li R, Grebe R, Bhutto I, Mu X, Lutty GA, 2012 The deletion of Math5 disrupts retinal blood vessel and glial development in mice. Exp Eye Res 96, 147–156. [PubMed: 22200487]

Frankfort BJ, Khan AK, Tse DY, Chung I, Pang JJ, Yang Z, Gross RL, Wu SM, 2013 Elevated intraocular pressure causes inner retinal dysfunction before cell loss in a mouse model of experimental glaucoma. Invest Ophthalmol Vis Sci 54, 762–770. [PubMed: 23221072]

Gregori NZ, Weiss MJ, Goldhardt R, Schiffman JC, Vega E, Mattis CA, Shi W, Kelley L, Hernandez V, Feuer WJ, 2014 Ocular decompression with cotton swabs lowers intraocular pressure elevation after intravitreal injection. J Glaucoma 23, 508–512. [PubMed: 23632408]

Hariprasad SM, Shah GK, Blinder KJ, 2006 Short-term intraocular pressure trends following intravitreal pegaptanib (Macugen) injection. Am J Ophthalmol 141, 200–201. [PubMed: 16387003]

He Z, Bui BV, Vingrys AJ, 2006 The rate of functional recovery from acute IOP elevation. Invest Ophthalmol Vis Sci 47, 4872–4880. [PubMed: 17065501]

He Z, Bui BV, Vingrys AJ, 2008 Effect of repeated IOP challenge on rat retinal function. Invest Ophthalmol Vis Sci 49, 3026–3034. [PubMed: 18326699]

Hoguet A, Chen PP, Junk AK, Mruthyunjaya P, Nouri-Mahdavi K, Radhakrishnan S, Takusagawa HL, Chen TC, 2019 The Effect of Anti-Vascular Endothelial Growth Factor Agents on Intraocular Pressure and Glaucoma: A Report by the American Academy of Ophthalmology. Ophthalmology 126, 611–622. [PubMed: 30472176]

Hong SW, Jee D, 2012 Effect of the Honan intraocular pressure reducer to prevent vitreous reflux after intravitreal bevacizumab injection. Eur J Ophthalmol 22, 615–619. [PubMed: 22562298]

Ivanova E, Muller U, Wassle H, 2006 Characterization of the glycinergic input to bipolar cells of the mouse retina. Eur J Neurosci 23, 350–364. [PubMed: 16420443]

Jia L, Cepurna WO, Johnson EC, Morrison JC, 2000 Effect of general anesthetics on IOP in rats with experimental aqueous outflow obstruction. Invest Ophthalmol Vis Sci 41, 3415–3419. [PubMed: 11006233]

Ke JB, Wang YV, Borghuis BG, Cembrowski MS, Riecke H, Kath WL, Demb JB, Singer JH, 2014 Adaptation to background light enables contrast coding at rod bipolar cell synapses. Neuron 81, 388–401. [PubMed: 24373883]

Knip MM, Valimaki J, 2012 Effects of pegaptanib injections on intraocular pressure with and without anterior chamber paracentesis: a prospective study. Acta Ophthalmol 90, 254–258. [PubMed: 20456259]

Kolb H, Famiglietti EV, 1974 Rod and cone pathways in the inner plexiform layer of cat retina. Science 186, 47–49. [PubMed: 4417736]

Kong YX, Crowston JG, Vingrys AJ, Trounce IA, Bui VB, 2009 Functional changes in the retina during and after acute intraocular pressure elevation in mice. Invest Ophthalmol Vis Sci 50, 5732–5740. [PubMed: 19643960]

Kurihara T, Kubota Y, Ozawa Y, Takubo K, Noda K, Simon MC, Johnson RS, Suematsu M, Tsubota K, Ishida S, Goda N, Suda T, Okano H, 2010 von Hippel-Lindau protein regulates transition from the fetal to the adult circulatory system in retina. Development 137, 1563–1571. [PubMed: 20388654]

Martinez-de-la-Casa JM, Ruiz-Calvo A, Saenz-Frances F, Reche-Frutos J, Calvo-Gonzalez C, Donate-Lopez J, Garcia-Feijoo J, 2012 Retinal nerve fiber layer thickness changes in patients with age-

related macular degeneration treated with intravitreal ranibizumab. Invest Ophthalmol Vis Sci 53, 6214–6218. [PubMed: 22915037]

Meister M, Pine J, Baylor DA, 1994 Multi-neuronal signals from the retina: acquisition and analysis. J Neurosci Methods 51, 95–106. [PubMed: 8189755]

Murray CD, Wood D, Allgar V, Walters G, Gale RP, 2014 Short-term intraocular pressure trends following intravitreal ranibizumab injections for neovascular age-related macular degeneration-the role of oral acetazolamide in protecting glaucoma patients. Eye (Lond) 28, 1218–1222. [PubMed: 25081290]

Okabe K, Kobayashi S, Yamada T, Kurihara T, Tai-Nagara I, Miyamoto T, Mukouyama YS, Sato TN, Suda T, Ema M, Kubota Y, 2014 Neurons limit angiogenesis by titrating VEGF in retina. Cell 159, 584–596. [PubMed: 25417109]

Pang CE, Mrejen S, Hoang QV, Sorenson JA, Freund KB, 2015a Association between Needle Size, Postinjection Reflux, and Intraocular Pressure Spikes after Intravitreal Injections. Retina 35, 1401–1406. [PubMed: 25650712]

Pang JJ, Abd-El-Barr MM, Gao F, Bramblett DE, Paul DL, Wu SM, 2007 Relative contributions of rod and cone bipolar cell inputs to AII amacrine cell light responses in the mouse retina. J Physiol 580, 397–410. [PubMed: 17255172]

Pang JJ, Frankfort BJ, Gross RL, Wu SM, 2015b Elevated intraocular pressure decreases response sensitivity of inner retinal neurons in experimental glaucoma mice. Proc Natl Acad Sci U S A 112, 2593–2598. [PubMed: 25675503]

Pang JJ, Gao F, Wu SM, 2004 Light-evoked current responses in rod bipolar cells, cone depolarizing bipolar cells and AII amacrine cells in dark-adapted mouse retina. J Physiol 558, 897–912. [PubMed: 15181169]

Rodriguez AR, de Sevilla Muller LP, Brecha NC, 2014 The RNA binding protein RBPMS is a selective marker of ganglion cells in the mammalian retina. J Comp Neurol 522, 1411–1443. [PubMed: 24318667]

Sabharwal J, Seilheimer RL, Cowan CS, Wu SM, 2016 The ON Crossover Circuitry Shapes Spatiotemporal Profile in the Center and Surround of Mouse OFF Retinal Ganglion Cells. Front Neural Circuits 10, 106. [PubMed: 28066192]

Sabharwal J, Seilheimer RL, Tao X, Cowan CS, Frankfort BJ, Wu SM, 2017 Elevated IOP alters the space-time profiles in the center and surround of both ON and OFF RGCs in mouse. Proc Natl Acad Sci U S A 114, 8859–8864. [PubMed: 28760976]

Sapieha P, Sirinyan M, Hamel D, Zaniolo K, Joyal JS, Cho JH, Honore JC, Kermorvant-Duchemin E, Varma DR, Tremblay S, Leduc M, Rihakova L, Hardy P, Klein WH, Mu X, Mamer O, Lachapelle P, Di Polo A, Beausejour C, Andelfinger G, Mitchell G, Sennlaub F, Chemtob S, 2008 The succinate receptor GPR91 in neurons has a major role in retinal angiogenesis. Nat Med 14, 1067–1076. [PubMed: 18836459]

Strettoi E, Dacheux RF, Raviola E, 1990 Synaptic connections of rod bipolar cells in the inner plexiform layer of the rabbit retina. J Comp Neurol 295, 449–466. [PubMed: 2351763]

Sun D, Bui BV, Vingrys AJ, Kalloniatis M, 2007 Alterations in photoreceptor-bipolar cell signaling following ischemia/reperfusion in the rat retina. J Comp Neurol 505, 131–146. [PubMed: 17729268]

Tah V, Orlans HO, Hyer J, Casswell E, Din N, Sri Shanmuganathan V, Ramskold L, Pasu S, 2015 Anti-VEGF Therapy and the Retina: An Update. J Ophthalmol 2015, 627674.

Tan B, MacLellan B, Mason E, Bizheva K, 2018 Structural, functional and blood perfusion changes in the rat retina associated with elevated intraocular pressure, measured simultaneously with a combined OCT+ERG system. PLoS One 13, e0193592.

Tao X, Sabharwal J, Seilheimer RL, Wu SM, Frankfort BJ, 2019 Mild Intraocular Pressure Elevation in Mice Reveals Distinct Retinal Ganglion Cell Functional Thresholds and Pressure-Dependent Properties. J Neurosci 39, 1881–1891. [PubMed: 30622167]

Thomas R, George R, Parikh R, Muliyil J, Jacob A, 2003 Five year risk of progression of primary angle closure suspects to primary angle closure: a population based study. Br J Ophthalmol 87, 450–454. [PubMed: 12642309]

Trexler EB, Li W, Massey SC, 2005 Simultaneous contribution of two rod pathways to AII amacrine and cone bipolar cell light responses. J Neurophysiol 93, 1476–1485. [PubMed: 15525810]

Tsai TI, Bui BV, Vingrys AJ, 2014 Effect of acute intraocular pressure challenge on rat retinal and cortical function. Invest Ophthalmol Vis Sci 55, 1067–1077. [PubMed: 24474280]

Uenoyama K, McDonald JS, Drance SM, 1969 The effect of intraocular pressure on visual electrical responses. Arch Ophthalmol 81, 722–729. [PubMed: 5781750]

Usui Y, Westenskow PD, Kurihara T, Aguilar E, Sakimoto S, Paris LP, Wittgrove C, Feitelberg D, Friedlander MS, Moreno SK, Dorrell MI, Friedlander M, 2015 Neurovascular crosstalk between interneurons and capillaries is required for vision. J Clin Invest 125, 2335–2346. [PubMed: 25915585]

van der Heijden ME, Shah P, Cowan CS, Yang Z, Wu SM, Frankfort BJ, 2016 Effects of Chronic and Acute Intraocular Pressure Elevation on Scotopic and Photopic Contrast Sensitivity in Mice. Invest Ophthalmol Vis Sci 57, 3077–3087. [PubMed: 27286365]

Highlights

We transiently elevated IOP to high levels in mice.

We assessed RGCs function at three time points after IOP elevation.

We assessed retinal vascular anatomy and RGC numbers at one time point after IOP elevation.

Multiple aspects of RGC function were abnormal after IOP elevation, and these had different patterns of recovery with time.

Specific retinal vascular plexi had reduced numbers of capillary branches.

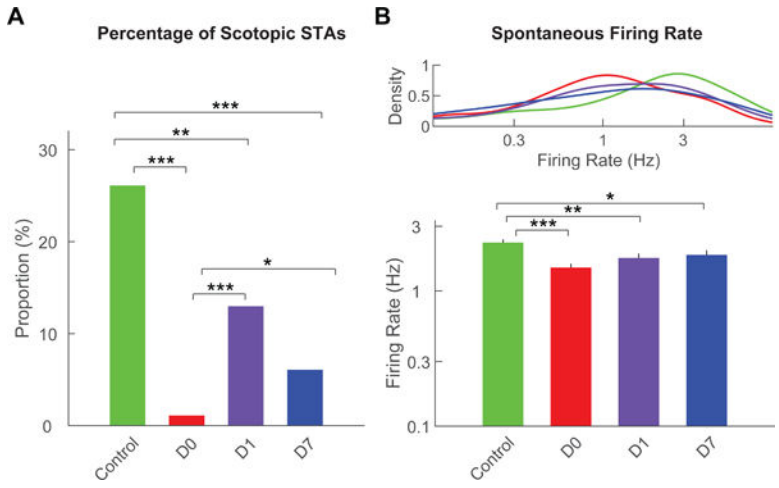

Figure 1. Presence of scotopic STAs and spontaneous firing rates.

(A) Percentage of RGCs that showed scotopic STAs from control eyes (green) or from treated eyes at D0 (red), D1 (purple) and D7 (blue). **(B)** Kernel density distributions (top) and averages (bottom) of spontaneous firing rates of RGCs from control eyes or from treated eyes at D0, D1 and D7. For all panels: *** = $p<0.001$; ** = $p<0.01$; * = $p<0.05$.

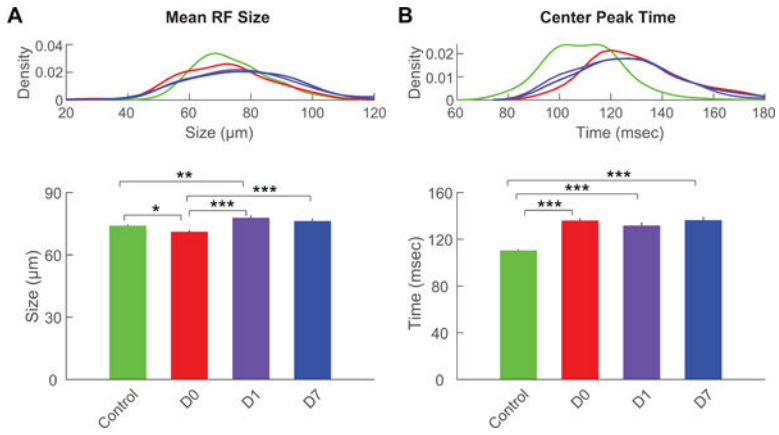

Figure 2. Center receptive field size and center STA peak time.

(A) Kernel density distributions (top) and averages (bottom) of receptive field size of RGCs from control eyes or from treated eyes at D0, D1 and D7. **(B)** Kernel density distributions (top) and averages (bottom) of center STA peak time of RGCs from control eyes or from treated eyes at D0, D1 and D7. Color scheme is the same as in Figure 1. For all panels: *** = $p<0.001$; ** = $p<0.01$; * = $p<0.05$.

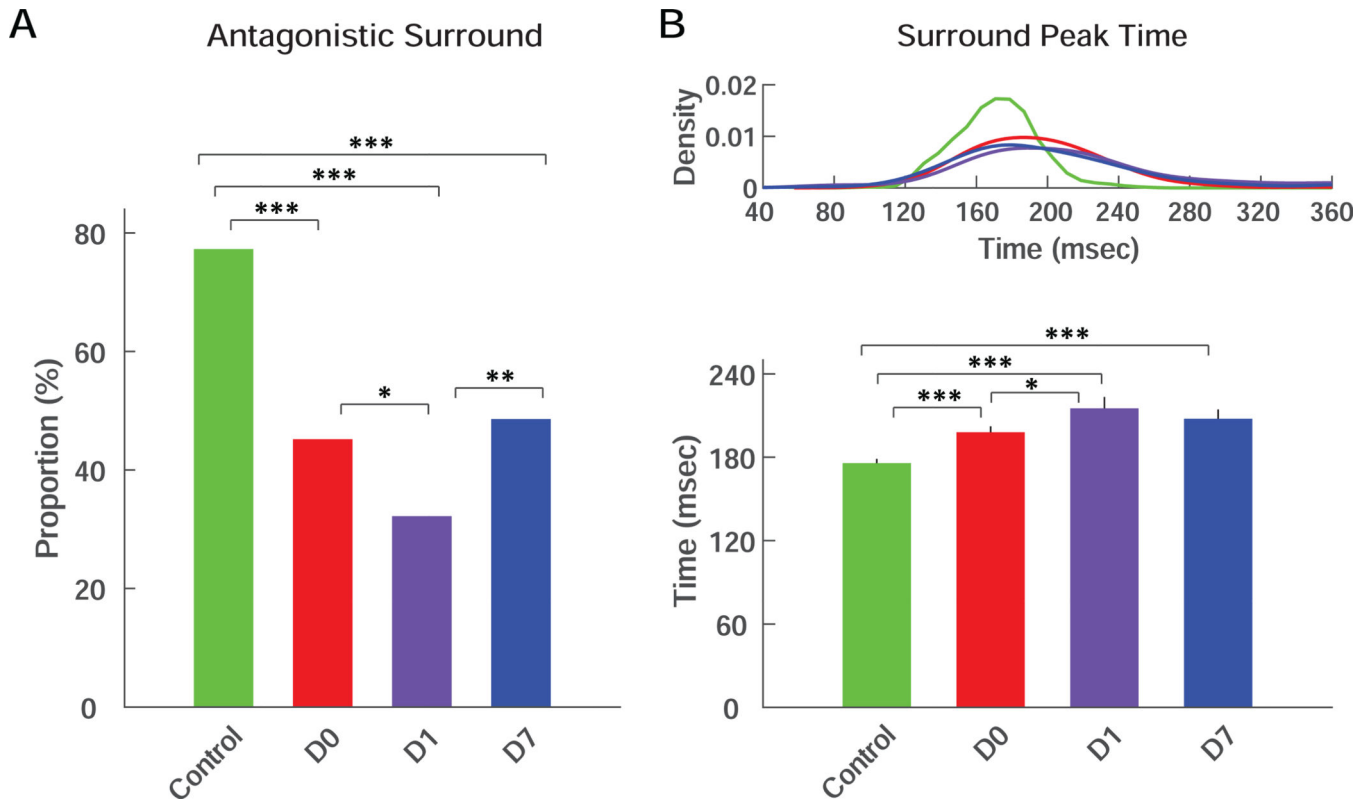

Figure 3. Presence of antagonistic surround and surround STA peak time.

(A) Percentage of the RGCs that showed antagonistic surround in RGCs from control eyes or from treated eyes at D0, D1 and D7. **(B)** Kernel density distributions (top) and averages (bottom) of surround STA peak time of RGCs from control eyes or from treated eyes at D0, D1 and D7. Only the RGCs that preserved their antagonistic surround were included. Color scheme is the same as in Figure 1. For all panels: *** = $p<0.001$; ** = $p<0.01$; * = $p<0.05$.

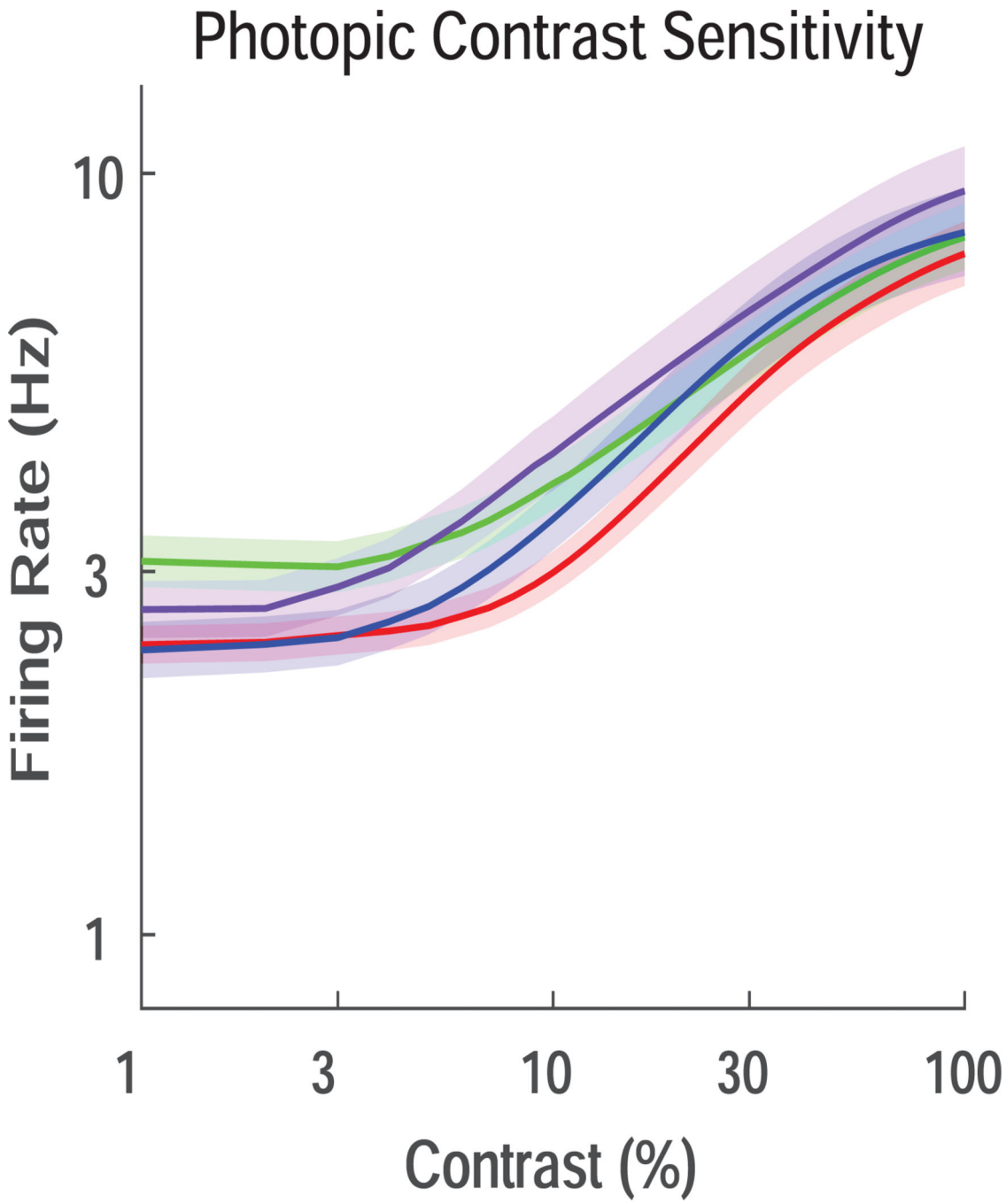

Figure 4. Photopic contrast sensitivity.

The firing rate of the RGCs was fit and plotted as a function of contrast for control RGCs (green) and RGCs after treatment (D0, red; D1, purple; D7, blue). No differences among groups were detected.

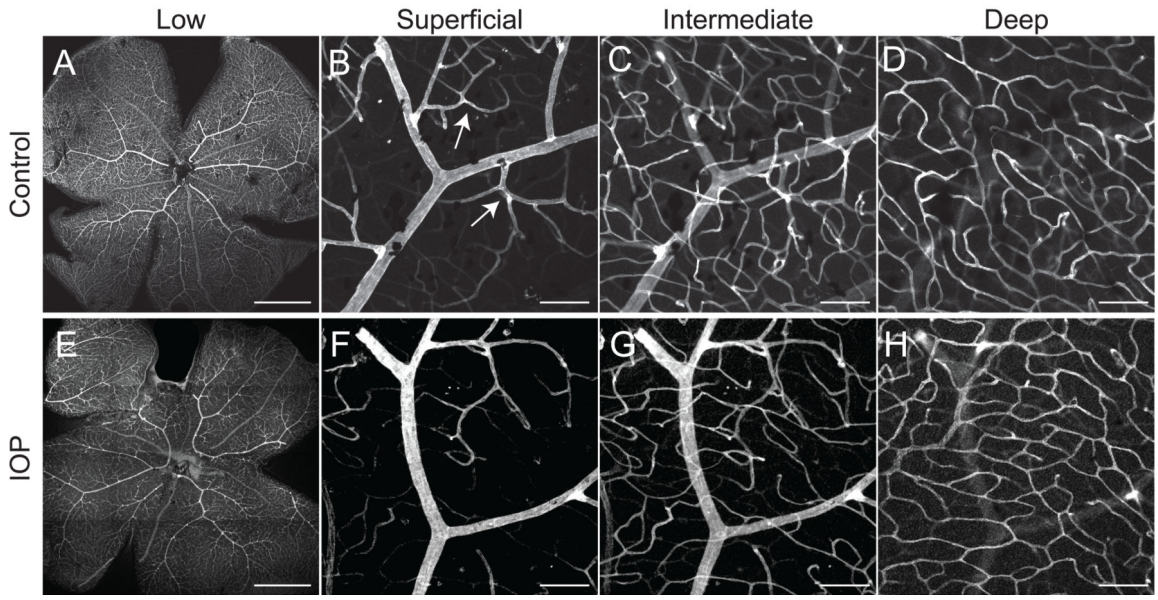

Figure 5. Retinal arterioles and capillary plexi.

Representative images of fluorescence conjugated Isolectin GS-IB_4 (*Griffonia simplicifolia*) identifies blood vessel walls in both Control (A-D) and IOP elevated (E-H) eyes. The arterioles (thicker branches, A and E), and the three vascular plexi (Superficial, B and F; Intermediate, C and G; and Deep, D and H) are detected with confocal microscopy. Examples of capillary branch points are shown in B (arrows). Scale bars: A and E = 1mm; B-D, F-H = 100 μm.

Table 1.

Pressure elevation following viscoelastic injection.

	Control	Pre	D0	D1	D7
Physiology experiments (mm Hg)	8.57 ± 0.34	8.79 ± 0.24	49.35 ± 1.35 ***	8.23 ± 0.30	8.18 ± 0.39
Vasculature Experiments (mm Hg)	9.32 ± 0.23	9.19 ± 0.77	51.88 ± 2.93 ***	9.07 ± 0.80	9.81± 0.63

Average IOP (mean ± SEM) before injection (Pre), immediately after injection (D0), 1 day after injection (D1) and 7 days after injection (D7). IOP on D0 was compared to other time points using a one way ANOVA.

*** $p<0.001$.

Table 2.

Number of retinas and RGCs in each group

	Control	D0	D1	D7
Retinas (N)	15	9	8	10
RGCs (N)	383	270	208	214

Table 3.

Effect of transient IOP elevation on retinal capillary plexus branching, arteriole diameter, and RGC number

	Superficial Plexus Branching	Intermediate Plexus Branching	Deep Plexus Branching	Arteriole Diameter	RGC Number
Control	105 ± 20%	103 ± 11%	103 ± 13%	103 ± 14%	108 ± 19%
IOP Elevation	82 ± 18% *	88 ± 14% *	98 ± 13%	108 ± 15%	106 ± 16%

Plexus branching, arteriole diameter, and RGC count are expressed as a ratio between the injected and uninjected eyes of the same animal (treated/untreated x 100% ± SD).

Multiple regions of the retina were sampled for each parameter (Methods).

* = $P < 0.05$.